Crystallization Behavior of the $CaO-Al_2O_3-MgO$ System Studied with a Confocal Laser Scanning Microscope

SUNG SUK JUNG and IL SOHN

The crystallization behavior of a calcium-aluminate system with various MgO content from 2.5 to 7.5 wt pct and CaO/Al_2O_3 ratios between 0.8 and 1.2 has been examined using a confocal laser scanning microscope (CLSM). CCT (continuous cooling transformation) and time temperature transformation (TTT) diagrams were constructed to identify the primary crystal phase of slag at different compositions and at cooling rates between 25 and 800 K/minutes. In the slag at a CaO/Al_2O_3 ratio of 1.0, crystallization temperature increased during isothermal and continuous cooling with higher MgO content, and the shortest incubation time was observed at 5 wt pct MgO. When MgO content was fixed to be 5 wt pct, crystallization temperature increased with lower CaO/Al_2O_3 ratio. According to the slag composition, cooling rates and temperature, the primary phase could be CA, or C_5A_3, or C_3A, or C_3MA_2, or MgO, and the crystal morphology changes from dendrites to faceted crystals to columnar crystals in this composition range.

DOI: 10.1007/s11663-012-9725-4

I. INTRODUCTION

THE reclamation of waste slag from ironmaking and steelmaking processes has allowed the steel industry to obtain additional revenue from this previously unvalued process waste. According to recent data, most of the blast furnace slags are recycled and used in either construction or roadside gravel. However, steelmaking process waste contain significant amounts of MgO, Al_2O_3, FeO, CaF_2 and other oxides and halides that limit its widespread use. Furthermore, the size and density of the cooled slags vary and can require additional crushing and separating that substantially increases the costs of recycling steelmaking slags. However, the strength and density of the cooled slags typically depend on the formation of crystalline phases, the ratio of the crystalline volume to the amorphous volume of the slag, and the morphology of the crystalline phases. Agarwal *et al.*[1] observed a significant increase in the cutting time for crystalline slags compared to glassy slags. Because the fraction of crystalline and amorphous slags during solidification and the crystal morphology are dependent upon the cooling rate, it is essential to provide fundamental information related to the crystallization characteristics of various slag systems to enable control of their eventual structure and composition. Furthermore, the crystallization of oxide slag is also an important topic in the control of radiative and conductive heat transfer in continuous casting.[2–4]

Ryu *et al.*[5] showed the effect of Al_2O_3 additions of up to 25 wt pct on crystallization in the $CaO-SiO_2-CaF_2$ system using a confocal laser scanning microscope (CLSM). The results indicated a change in the crystalline phase from $3CaO \cdot 2SiO_2 \cdot CaF_2$ to $2CaO \cdot SiO_2 \cdot Al_2O_3$ as the SiO_2 was replaced with Al_2O_3. Al_2O_3 addition also increased the crystallization temperature of the melt and shortened the incubation time of the crystallization, as indicated by the time temperature transformation (TTT) diagram. Zhang *et al.*[6] also observed the crystallization behavior in mold fluxes with varying Al_2O_3/SiO_2 ratios using a CLSM and observed that the crystallization temperature increased with increasing Al_2O_3/SiO_2. Thus, depending on the chemical composition of the melt and the cooling conditions, distinct differences in the primary crystal phases and the morphology were observed. In a more recent study by Heulens *et al.*[7], isothermal crystallization in the $CaO-Al_2O_3-SiO_2$ system was accelerated by wöllastonite particles, which resulted in a faceted crystal being observed at 1643 K (1370 °C) and a dendritic non-faceted crystal being observed at 1593 K (1320 °C).

Engstrom *et al.*[8] analyzed slag samples from commercial basic oxygen furnace (BOF) and EAF (electric arc furnace) plants that were cooled at various rates ranging from 0.3 to 500 K/s using MgO crucible cooling and water granulation cooling, in which uniformly fine meta-stable phases formed during rapid cooling. Using X-ray diffraction (XRD) and scanning electron microscope (SEM) analyses, differences were observed in the particle size distribution due to the different cooling rates and crystal phases, including β-dicalcium silicate (β-$2CaO \cdot SiO_2$) and calcium ferrite ($2CaO \cdot Fe_2O_3$), which determined the physical properties of the slag after solidification. Tossavainen *et al.*[9] also characterized various slag through semi-rapid cooling in crucibles and rapid cooling by water granulation, and studied the effect of different cooling conditions on the melt stability. Ladle slags of CaO-14.2 wt pct SiO_2-12.6 wt pct MgO-22.9 wt pct Al_2O_3 that were rapidly

SUNG SUK JUNG, Graduate Student, and IL SOHN, Associate Professor, are with the Materials Science and Engineering, Yonsei University, 50 Yonsei-ro, Seodaemun-gu, Seoul 120-749, Korea Contact e-mail: ilsohn@yonsei.ac.kr

Manuscript submitted April 21, 2012.
Article published online September 1, 2012.

quenched, which consisted of 98 pct glass and 2 pct crystallization, showed the highest volume stability.

Kashiwaya *et al.*[10] developed the double hot thermocouple technique (DHTT), which is similar to a CLSM, for *in situ* observation and measurement of mold slag crystallization. The shape and the mode of crystal growth were quite different between the isothermal experiment for TTT diagrams and the non-isothermal experiment for CCT (continuous cooling transformation) diagrams. CaO-SiO_2-7 wt pct Al_2O_3-5 wt pct Na_2O slags that were isothermally held at 1573 K and 1413 K (1300 °C and 1140 °C), respectively, showed an equiaxed dendrite and a cubic crystal, respectively. Similar work performed by Mutale *et al.*[11] in CaO-SiO_2-6 wt pct Al_2O_3-2 wt pct Na_2O slag showed a double-nose TTT diagram, where high-temperature dicalcium silicate ($2CaO \cdot SiO_2$) was observed at 1423 K (1150 °C) (upper nose) and tricalcium silicate ($3CaO \cdot SiO_2$) was observed at 1323 K (1050 °C) (lower nose).

In this study, the crystallization behavior of CaO-Al_2O_3-MgO slag, which form the major constituent of steelmaking ladle slags, was investigated at various compositions using a CLSM. The slag was cooled at various rates, and the CCT/TTT diagrams were constructed. To qualitatively identify the primary phases during solidification, quenched melt samples were analyzed using SEM-EDS (scanning electron microscope-energy dispersive spectroscopy) and XRD.

II. EXPERIMENTAL

A. *Preparation of Samples*

Reagent-grade $CaCO_3$, Al_2O_3, and MgO were used to produce the slag composition given in Table I. The chemicals were mixed and premelted at 1773 K (1500 °C) for 3 hours under 0.4 L/minutes of high-purity Ar (99.999 pct) in a Pt-10 wt pct Rh crucible to calcinate the carbonates and to obtain a homogeneous sample of CaO-Al_2O_3-MgO. The homogenized samples were quenched on a water-cooled copper plate and crushed for the primary experiments using the CLSM. The chemical composition of the slag was analyzed using X-ray fluorescence (XRF) spectroscopy (S4 Explorer; Bruker AXS GmbH, Karlsruhe, Germany). The pre- and post-experimental XRF analyses revealed negligible changes in the chemical composition. Thus, the composition based on the initial weighed quantities was taken as the chemical composition throughout the study.

B. *Experimental Apparatus and Procedure*

Approximately 0.06 g of the master slag sample was placed in a Pt-10 wt pct Rh crucible with a diameter of 0.5 cm and a height of 0.5 cm. This small amount of slag allowed the formation of a consistent thin layer of slag that covered the Pt-10 wt pct Rh crucible. *In situ* observation of the crystallization was performed using a halogen lamp heating stage and a CLSM (SVF-SP; Yonekura MFG. Co. LTD, Japan), as depicted in Figure 1. The halogen lamp irradiates light toward the gold-coated surface of the reaction chamber that reflects the energy towards the focal plane of the crucible to rapidly heat the slag sample. After the sample reached thermal equilibrium, the melt was cooled at a controlled rate, and video images of the molten slag were collected during the non-isothermal and isothermal cooling sequence. Some CLSM images have been digitally enhanced using Adobe Photoshop® to increase the image clarity. The temperature and time were documented at the onset of crystallization, and this information was later used to construct CCT and TTT diagrams. Isothermal holding temperatures for the TTT diagram were rapidly reached by cooling to the desired target temperature at 800 K/minutes.

Table I. Composition of Premelted Slag Samples Analyzed by XRF

No.	Chemical Constituents			
	Wt Pct CaO	Wt Pct Al_2O_3	Wt Pct MgO	CaO/Al_2O_3
Sample 1	43.2	52.2	4.6	OS
Sample 2	48.6	46.1	4.9	1.0
Sample 3	51.6	43.2	4.7	1.2
Sample 4	49.8	47.8	2.4	1.0
Sample 5	47.2	45.4	7.4	1.0

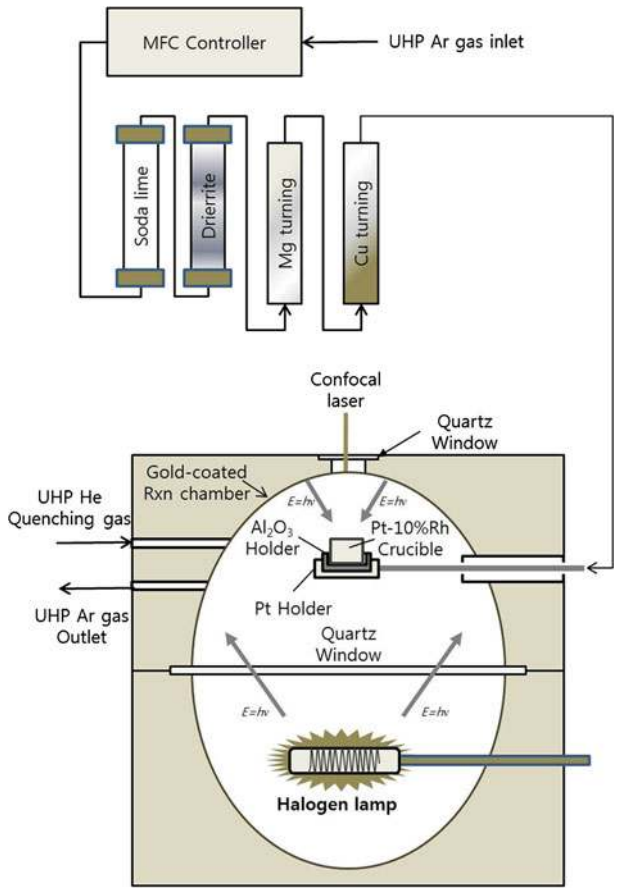

Fig. 1—Schematic diagram of the CLSM.

A flow of 0.2 lpm of UHP Ar (99.9999 pct) was passed into the reaction chamber for approximately 15 minutes prior to and during the experiment. The gas was deoxidized before use with heated columns of Mg and Cu turnings. Preliminary experiments with slag samples showed the maximum possible heating rate to be 1000 K/minutes, and the controllable cooling rate without quenching gases could be varied from 3 to 800 K/minutes. Nucleation and growth of the crystals with various slag compositions were observed by continuously cooling the slag at fixed rates from 25 to 800 K/minutes and by isothermal cooling at various target temperatures.

To identify the crystalline phases during isothermal cooling, slags were solidified at the onset of nucleation. The slags were cooled by a separate He gas cooling line connected to the gold-coated reaction chamber with a 0.3 lpm flow of He gas at the initiation of crystallization. Cooling rates of more than 3000 K/minutes have been possible using a He quenching gas in a CLSM. The rapidly cooled sample was then mounted, polished, and analyzed by SEM-EDS (JSM-6700F; JEOL, Japan). Phase identification of the various quenched slags was performed through XRD (Ultima; Rigaku, Japan) analysis.

III. RESULTS

A. *Effect of MgO Addition on the Crystal Morphology of CaO-Al_2O_3-Based Slag*

The effect on crystallization behavior of the CaO-Al_2O_3-based slag at a fixed CaO/Al_2O_3 ratio of 1.0 with MgO additions from 2.5 to 7.5 wt pct and at various cooling rates was determined. Figure 2 shows the CLSM images when the slag was continuously cooled at a constant rate of 25 K/minutes. The onset of the nucleation and growth of primary crystals in the CaO-Al_2O_3-5 wt pct MgO slag in Figure 2(b) showed faceted crystals followed by columnar growth from the surface, while the CaO-Al_2O_3-2.5 wt pct MgO sample initiated its crystallization with the fast growth of dendrites as in Figure 2(a) and the CaO-Al_2O_3-7.5 wt pct MgO sample showed relatively slow growth of dendrites into the undercooled melt, resulting in a star-like shape as in Figure 2(c). The same morphology of crystallization was found when continuously cooled at a constant rate of 100 K/minutes. Cooling rates from 400 to 800 K/minutes showed small non-faceted spheroidal nodules rapidly forming and fully solidifying in the undercooled melt provided in later sections.

The primary crystal morphologies that occur during isothermal cooling of calcium-aluminate slag with 2.5, 5 and 7.5 wt pct MgO and a CaO/Al_2O_3 ratio of 1.0 are shown in Figure 3. Dendritic primary crystals in Figure 3(a) were observed between 1493 K and 1523 K (1220 °C and 1250 °C) when MgO content was 2.5 wt pct. With 5 wt pct MgO, hexagonally faceted crystals were observed at 1523 K and 1533 K (1250 °C and 1260 °C), as shown in Figure 3(b). For calcium-aluminate slags with 7.5 wt pct MgO, the primary crystal morphology when the slags were isothermally cooled at temperatures between 1543 K and 1593 K (1270 °C and 1320 °C) was observed to be dendrites, with no faceted crystals formed.

B. *Effect of CaO/Al_2O_3 Ratio on the Crystal Morphology of CaO-Al_2O_3-Based Slag*

The primary crystal morphologies that occur during isothermal cooling of calcium-aluminate slag with 5 wt pct MgO and various CaO/Al_2O_3 ratios are shown in Figure 4. A non-equiaxed dendritic morphology is observed for a CaO/Al_2O_3 ratio of 0.8 in Figure 4(a), and an equiaxed dendritic morphology is observed for a CaO/Al_2O_3 ratio of 1.2 in Figure 4(c). An hexagonally faceted crystal similar to Figure 3(b) is shown in Figure 4(b).

C. *Effect of MgO on the Non-Isothermal and Isothermal Cooling Diagrams in CaO-Al_2O_3-Based Slag*

The CCT diagrams of the CaO-Al_2O_3-based slag with 2.5, 5 and 7.5 wt pct MgO and a constant CaO/Al_2O_3 ratio of 1 are shown in Figure 5 for cooling rates of 25, 50, 100, 400, and 800 K/minutes, initiated from 1843 K (1570 °C). The results showed that higher concentrations of MgO increased the crystallization starting temperature when the cooling rates were not more than 100 K/minutes. For cooling rates of 400 K/minutes and above with 5.0 and 7.5 wt pct MgO, increased MgO addition to the slag had relatively little effect, while no crystal phase was observed for 2.5 wt pct MgO.

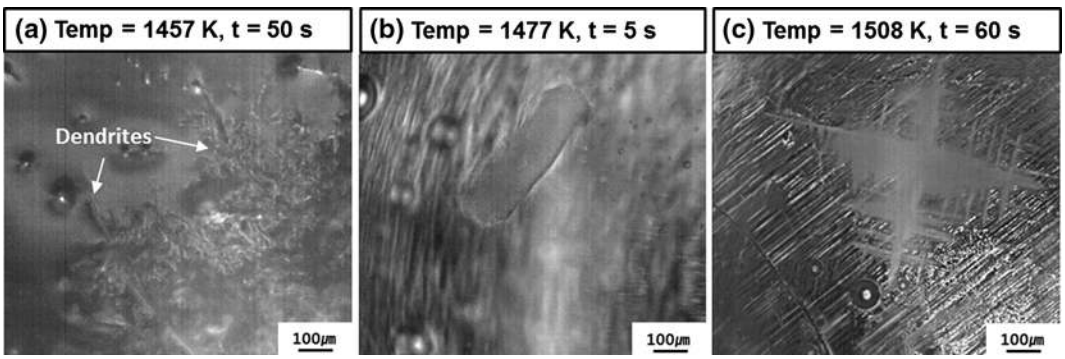

Fig. 2—CLSM image of crystallization when continuously cooled at 25 K/min in the calcium-aluminate-based slags at a fixed CaO/Al_2O_3 ratio of 1.0 containing (*a*) 2.5 wt pct MgO, $t = 50$ s (*b*) 5 wt pct MgO, $t = 5$ s and (*c*) 7.5 wt pct MgO, $t = 60$ s.

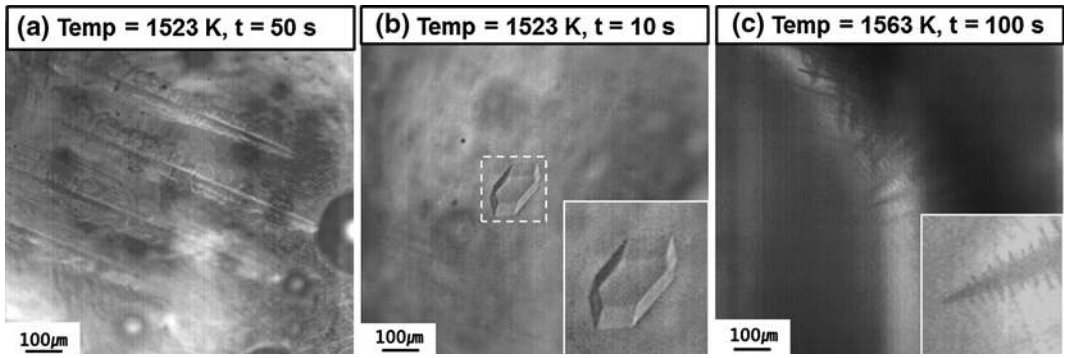

Fig. 3—CLSM image of crystallization for isothermally cooled calcium-aluminate-based slags at fixed CaO/Al_2O_3 of 1.0 containing (*a*) 2.5 wt pct MgO at 1523 K (1220 °C), t = 50 s (*b*) 5 wt pct MgO at 1523 K (1220 °C), t = 10 s and (*c*) 7.5 wt pct MgO at 1563 K (1290 °C), t = 100 s.

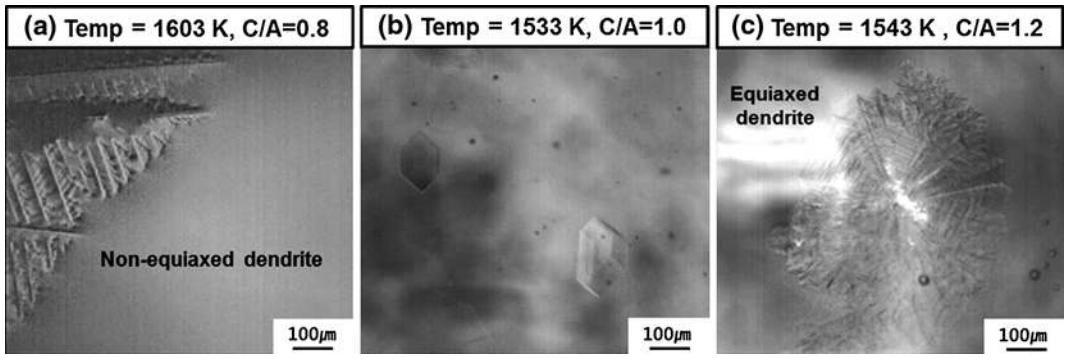

Fig. 4—CLSM image of crystallization for isothermally cooled calcium-aluminate-based slags containing 5 wt pct MgO and a CaO/Al_2O_3 ratio of (*a*) 0.8, (*b*) 1.0 and (*c*) 1.2.

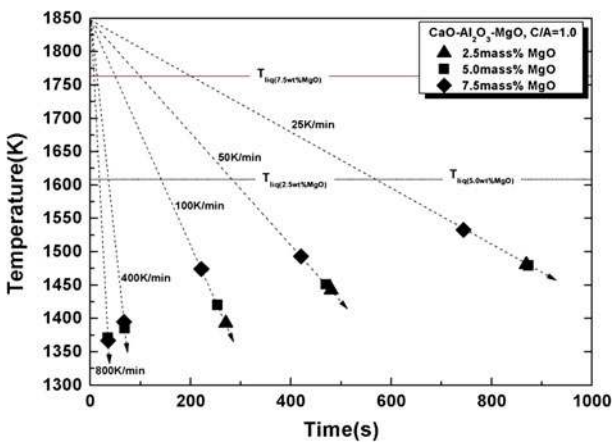

Fig. 5—Non-isothermal CCT diagram for the calcium-aluminate-based slags containing 2.5, 5 and 7.5 wt pct MgO at a CaO/Al_2O_3 ratio of 1.0.

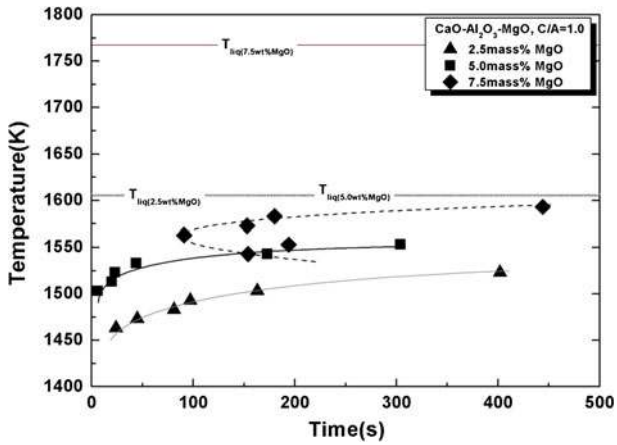

Fig. 6—Isothermal TTT diagram for the calcium-aluminate-based slags containing 2.5, 5 and 7.5 wt pct MgO at a CaO/Al_2O_3 ratio of 1.0.

The isothermal cooling TTT diagrams for the CaO-Al_2O_3-based slag containing different amount of MgO and a constant CaO/Al_2O_3 ratio of 1 are shown in Figure 6. Whereas the 7.5 wt pct MgO-containing CaO-Al_2O_3-based slag showed a typical 'C'-shaped TTT curve, the 2.5 and 5 wt pct MgO-containing CaO-Al_2O_3-based slag showed a half-'C'-shaped TTT curve. The nose, or the critical minimum time required to form a given degree of crystallization,[10] is often analyzed to qualitatively compare the tendency for crystallization and the effects of various chemical compositions of slag systems. In the CaO-Al_2O_3-7.5 wt pct MgO slag, the TTT diagram was "C" shaped, and the apparent nose of the TTT could be considered to fall approximately at 1563 K (1290 °C) and 91 seconds. As the MgO content increased from 5 to 7.5 wt pct, the nose temperature and the critical time for nucleation increased. Furthermore, the minimum undercooling needed for crystallization during isothermal

Table II. Critical Cooling Rates (R_C) Calculated from Eq. [1] and the TTT Diagram for the CaO-Al_2O_3-MgO Slag System

CaO/Al_2O_3	MgO (Wt Pct)	$T_{Initial}$ [K (°C)]	$T_{Critical}$ [K (°C)]	$t_{Critical}$ (s)	R_C (K/min)
0.8	5	1843 (1570)	1603 (1330)	39	369
1	5	1843 (1570)	1503 (1230)	6	3400
1.2	5	1843 (1570)	1523 (1250)	15	1280
1	2.5	1843 (1570)	1463 (1190)	24	950
1	7.5	1843 (1570)	1563 (1290)	91	185

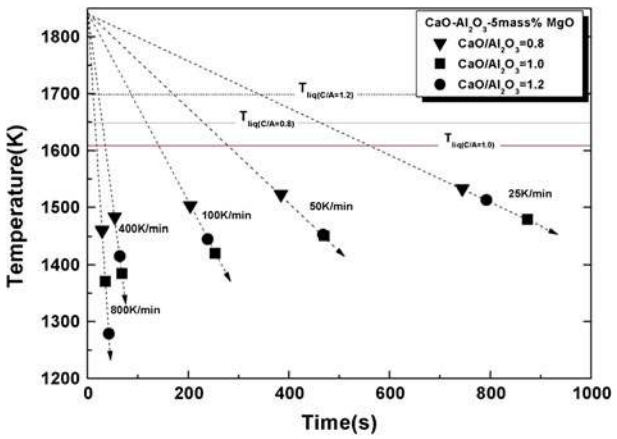

Fig. 7—Non-isothermal CCT diagram for the calcium-aluminate-based slags of various CaO/Al_2O_3 at 5 wt pct MgO.

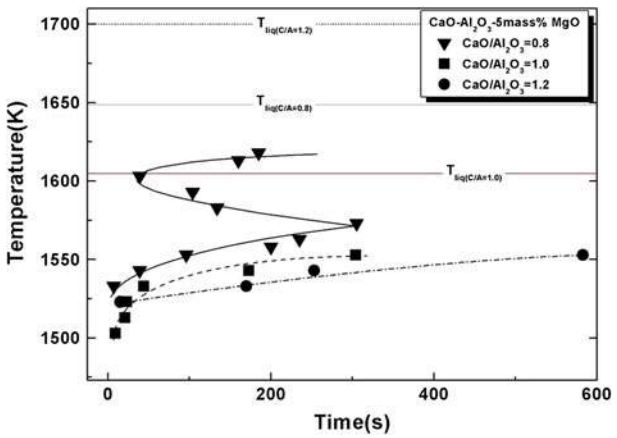

Fig. 8—Isothermal TTT diagram for the calcium-aluminate-based slags of various CaO/Al_2O_3 ratios with 5 wt pct MgO.

cooling was found to be 85 K, 57 K, and 175 K for the 2.5, 5 and 7.5 wt pct MgO-containing slags, respectively. Using the nose of the TTT diagram, the critical cooling rate (R_C) as defined by Yinnon *et al.*[12] is expressed by Eq. [1], which can be used to compare the crystallization behavior at various slag compositions.

$$R_C = (T_{Intial} - T_{Critical})/t_{critical} \quad [1]$$

where, $T_{Initial}$ (K) is the initial temperature before cooling, $T_{Critical}$ (K) is the temperature at the nose, and $t_{Critical}$ (seconds) is the time at $T_{Critical}$. The calculated values of the critical cooling rates for the various slag compositions are given in Table II. For the CaO-Al_2O_3-7.5 wt pct MgO melt with a CaO/Al_2O_3 ratio of 1.0, R_C was 185 K/minutes, which suggests that cooling rates above this value will likely result in an amorphous structure. However, results in Figure 5 indicate crystallization occurring at cooling rates of 400 and 800 K/minutes. For the CaO-Al_2O_3-5 wt pct MgO slag with a CaO/Al_2O_3 ratio of 1.0, R_C was 3400 K/minutes.

D. *Effect of the CaO/Al_2O_3 Ratio on the Non-Isothermal and Isothermal Cooling Diagrams in the CaO-Al_2O_3-5 wt pct MgO Slag*

The effect of CaO/Al_2O_3 ratios between 0.8 and 1.2 in slags containing 5 wt pct MgO on the non-isothermal CCT diagram is shown in Figure 7. The resulting CCT diagram indicates the crystallization temperatures to be highest for a CaO/Al_2O_3 ratio of 0.8, followed by CaO/Al_2O_3 ratios of 1.2 and 1.0.

The effect of CaO/Al_2O_3 ratios between 0.8 and 1.2 in slags containing 5 wt pct MgO on the isothermal TTT diagram is shown in Figure 8. The resulting TTT diagram indicates that the crystallization temperatures are the highest for a CaO/Al_2O_3 ratio of 0.8, and the double nose indicates that different crystal phases are likely to occur in the top "C"-shaped curve than in the bottom "C"-shaped curve. The TTT diagram changes significantly with higher CaO/Al_2O_3 ratios. The double nose disappears for the TTT diagrams with CaO/Al_2O_3 ratios of 1.0 and 1.2, which likely results in the formation of a single primary crystal phase during isothermal cooling. The initial crystallization temperatures are much lower for slags with CaO/Al_2O_3 ratios of 1.0 and 1.2 than for a ratio of 0.8.

E. *SEM-EDS Morphological Observations and Compositional Measurements of Solidified Slags*

In order to determine the crystal phase, the slag was quenched within the confocal chamber with the cooling gas at the onset of crystallization in preparation for SEM and XRD. Figure 9 shows dendritic crystals in the melt of a slag with a CaO/Al_2O_3 ratio of 0.8 with 5 wt pct of MgO at two different nose temperatures, 1543 K and 1603 K (1270 °C and 1330 °C). The slag isothermally held at 1603 K (1330 °C) showed needle-like dendrites and the slag at 1543 K (1270 °C) showed cellular dendrites. Figure 10 presents results for slag with various compositions that were continuously cooled at 800 K/minutes. Uniform finely dispersed crystallization was observed for slag containing 5 wt pct MgO. The morphology was spherical nodules (Figure 10(a)) at a CaO/Al_2O_3 ratio of 0.8, which changed to a dendritic structure (Figure 10(c)) at a CaO/Al_2O_3 ratio of 1.2. Slag with 7.5 wt pct MgO (Figure 10(d)) showed large, separated regions of amorphous-only morphology during continuous cooling. The EDS analyses of the crystalline phases of the as-quenched samples have been plotted in a ternary phase diagram, as shown in Figure 11, and the values lie mostly inside an enclosed area where C_3MA_2, C_3A and $C_{12}A_7$ may exist.

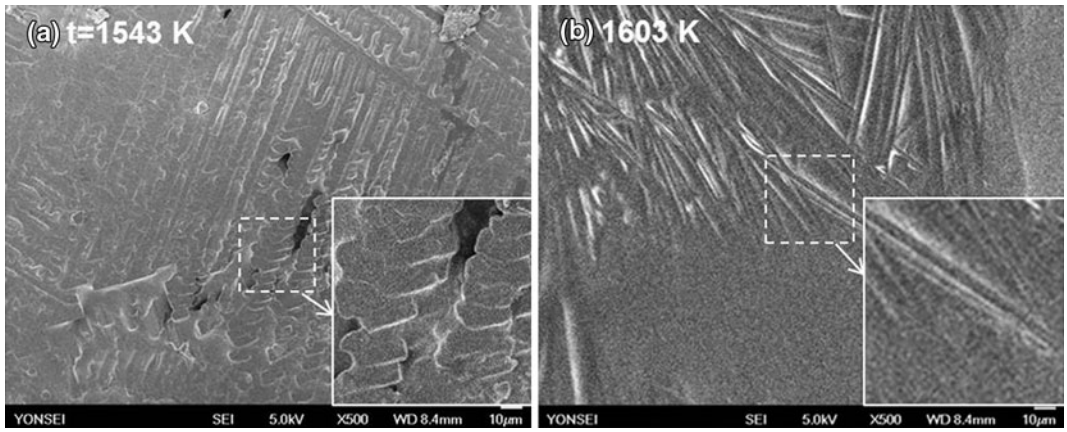

Fig. 9—SEM images of the crystal phases in the slag with a CaO/Al_2O_3 ratio of 0.8 and 5 wt pct MgO (*a*) at 1543 K (1270 °C) and (b) at 1603 K (1330 °C).

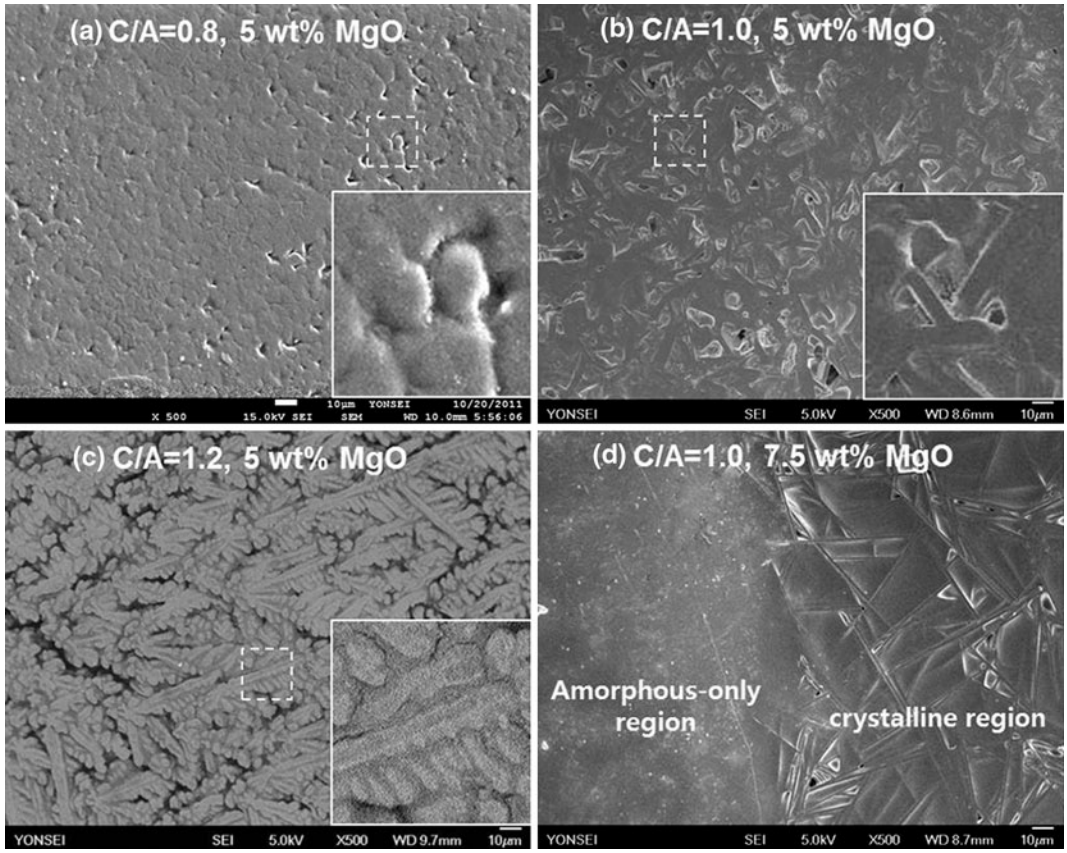

Fig. 10—SEM image of crystallized $CaO\text{-}Al_2O_3\text{-}MgO$ slags cooled at 800 K/min when (*a*) CaO/Al_2O_3 = 0.8, 5 wt pct MgO, (*b*) CaO/Al_2O_3 = 1.0, 5 wt pct MgO, (*c*) CaO/Al_2O_3 = 1.2, 5 wt pct MgO and (*d*) CaO/Al_2O_3 = 1.0, 7.5 wt pct MgO.

The initial composition of the slag is marked with an asterisk. However, the EDS results are qualitative and do not provide definitive evidence to identify the slag system, so additional analyses with XRD were performed.

F. *XRD Analyses of Crystalline Phases Within the $CaO\text{-}Al_2O_3\text{-}MgO$ Slag*

XRD analyses of quenched samples cooled at various rates and with different compositions were performed. Prior EDS data suggested several phase candidates for each sample within the phase diagram.

Figure 12(a) shows the XRD analyses for specimens with a CaO/Al_2O_3 ratio of 0.8 with 5 wt pct MgO that were isothermally cooled at 1543 K and 1603 K (1270 °C and 1330 °C), which exhibited a double "C"-shaped TTT diagram. For the upper "C," the XRD patterns suggest that the CA phase was dominant in the sample isothermally cooled at 1603 K (1330 °C), while the C_5A_3 phase was dominant in the sample for the lower "C" treated at

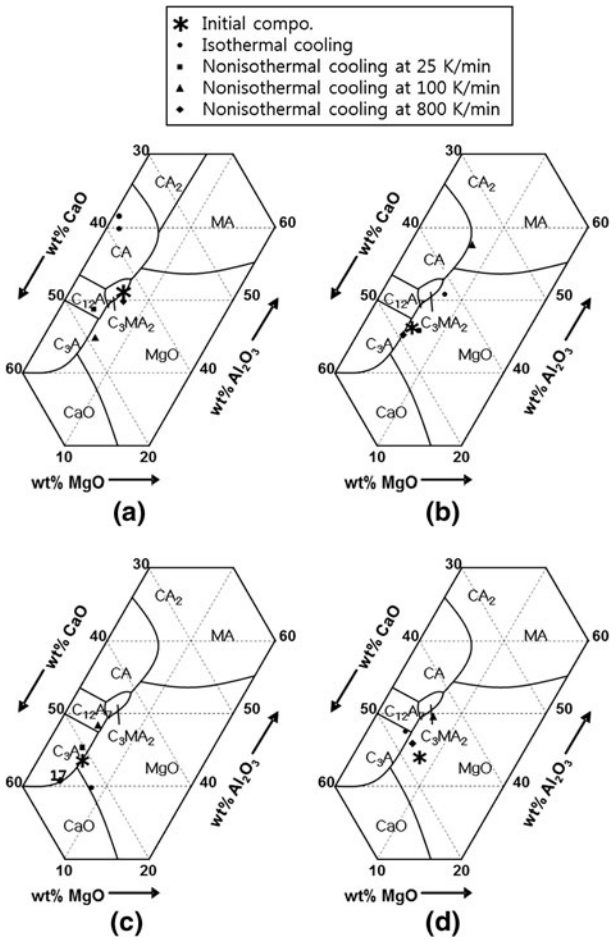

Fig. 11—Part of the CaO-Al_2O_3-MgO phase diagram that depicts the approximate composition of the phases with an initial composition of (*a*) C/A = 0.8 and 5 wt pct MgO, (*b*) C/A = 1.0 and 5 wt pct MgO, (*c*) C/A = 1.2 and 5 wt pct MgO and (*d*) C/A = 1.0 and 7.5 wt pct MgO.

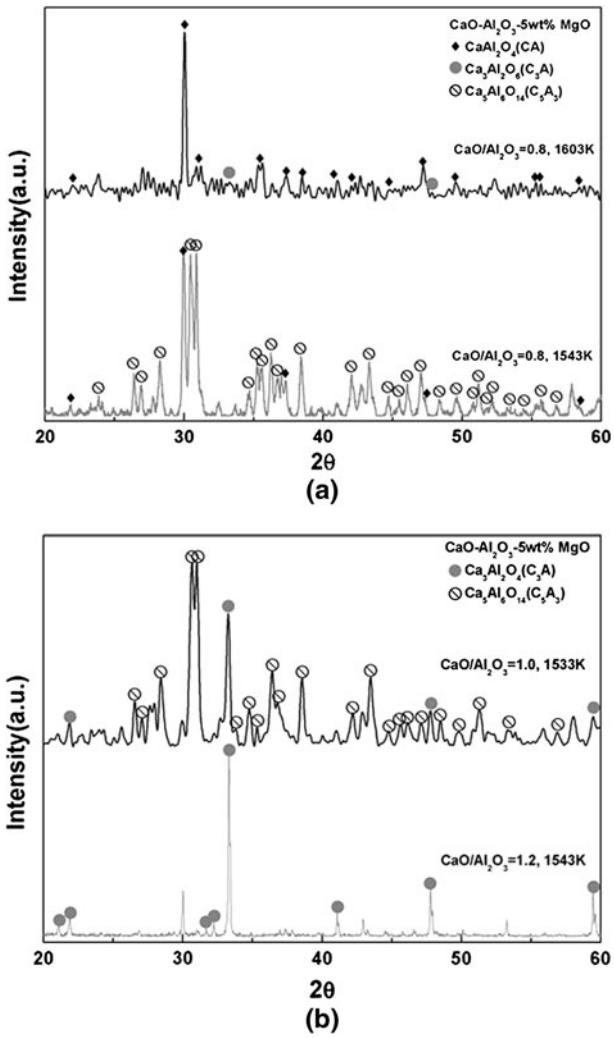

Fig. 12—XRD patterns of crystallized calcium-aluminate slag at a (*a*) CaO/Al_2O_3 ratio of 0.8 with 5 wt pct MgO isothermally cooled at 1543 K and 1603 K (1270 °C and 1330 °C), and (*b*) CaO/Al_2O_3 ratio of 1.0 and 1.2, and 5 wt pct MgO isothermally cooled at 1533 K and 1543 K (1260 °C and 1270 °C), respectively.

1543 K (1270 °C). At 1603 K (1330 °C), the CA phase emerges as the primary phase, while the C_3A phase appears later as a secondary phase. At 1543 K (1270 °C), the C_5A_3 phase is the primary phase, while the CA phase appears later as a secondary phase. The XRD peaks in Figure 12(b) show C_5A_3 and C_3A to be the primary phases precipitated in the slag with CaO/Al_2O_3 ratios of 1.0 and 1.2 with 5 wt pct MgO, when cooled at 1533 K and 1543 K (1260 °C and 1270 °C), respectively. However, specimens with CaO/Al_2O_3 ratios from 0.8 to 1.0, when continuously cooled, showed C_3MA_2 to be the primary phase that was initially formed at high temperatures, as shown by the XRD results given in Figure 13, and subsequent secondary phases formed during further cooling. At a CaO/Al_2O_3 ratio of 1.2 and 5 wt pct MgO, the dominant characteristic peak for samples cooled at 800 K/minutes appeared to be C_3A, and subsequent secondary phases of C_3MA_2 were formed. In Figure 14(a), C_3A is considered the primary phase with secondary phases of CA and C_5A_3 when cooled at 25 K/minutes. The CA phase was not found, but the C_5A_3 phase becomes more apparent. Corresponding to the CCT diagram, the XRD pattern shows that this slag becomes amorphous when cooled at 800 K/minutes. In Figure 14(b), MgO phase was found to be the primary phase in the slag of CaO/Al_2O_3 of 1.0 and 7.5 wt pct MgO at 25 K/minutes with C_5A_3 as the secondary phase. This C_5A_3 peak becomes less apparent at higher cooling rates.

IV. DISCUSSION

A. *Crystallization of the Primary Phase*

The results of the XRD and SEM analyses show the observed primary phases to be in good agreement with the phases expected from the CaO-Al_2O_3-MgO ternary phase diagram. The specimens with CaO/Al_2O_3 ratios of 0.8 and 1.0 and 5 wt pct MgO result in $Ca_3MgAl_4O_{10}$ (C_3MA_2) as the primary phase during continuous cooling,[13] while $CaAl_2O_4$ (CA) was found to be the primary phase when slag with a CaO/Al_2O_3 ratio of 0.8 and 5 wt pct MgO were isothermally cooled at 1603 K (1330 °C). At 1543 K

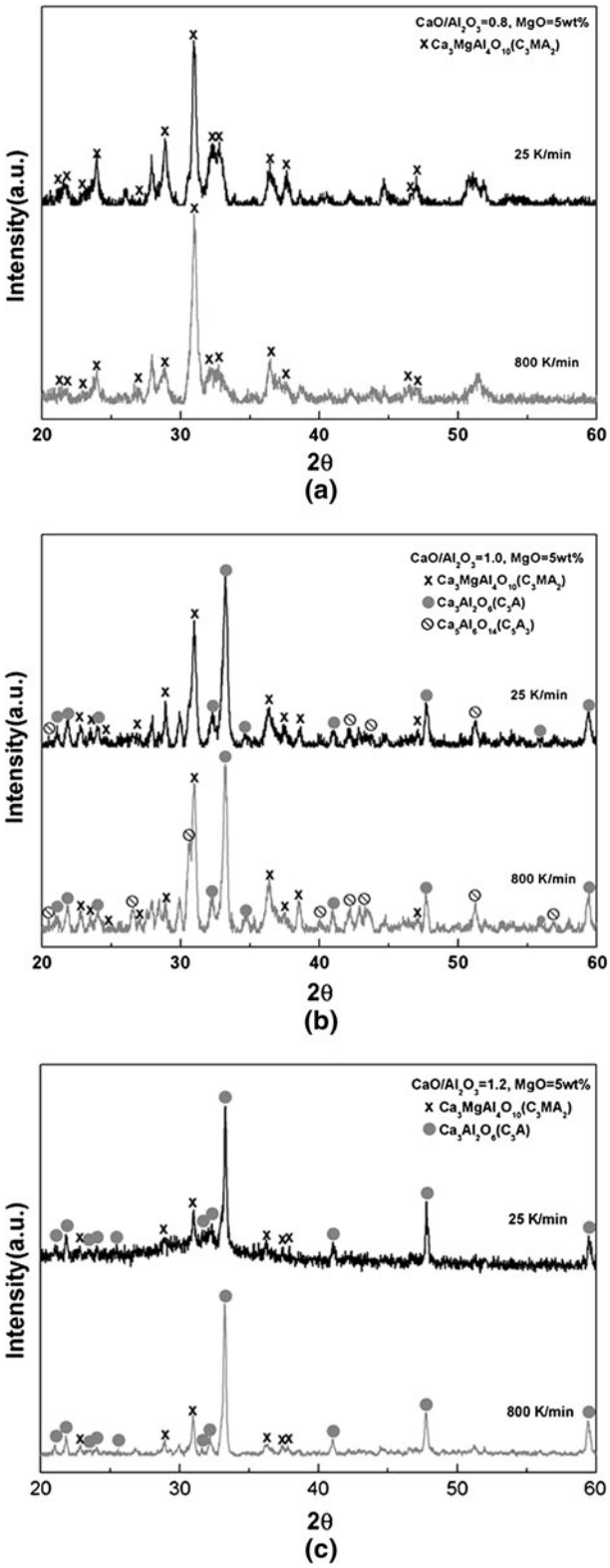

Fig. 13—XRD patterns of slags with 5 wt pct MgO cooled at 25 and 800 K/min at (*a*) a CaO/Al_2O_3 ratio of 0.8, (*b*) a CaO/Al_2O_3 ratio of 1.0, and (*c*) a CaO/Al_2O_3 ratio of 1.2.

(1270 °C), the meta-stable C_5A_3 phase[14] was observed. This phase may be the dominant phase in the low-temperature regime of the lower nose. According to

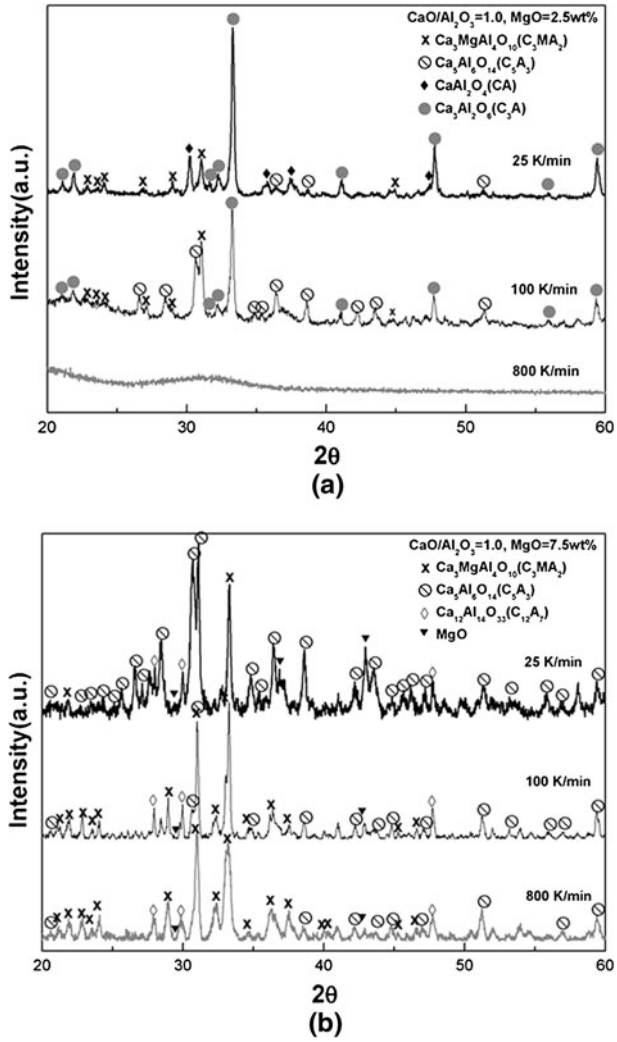

Fig. 14—XRD patterns of slags at a CaO/Al_2O_3 ratio of 1.0 cooled at 25, 100 and 800 K/min with MgO content of (*a*) 2.5 wt pct and (*b*) 7.5 wt pct.

Hagen *et al.*,[15] major portion of the synthesized $C_{12}A_7$ with a CaO/Al_2O_3 ratio of 0.94 cooled at 50 K/h changed into the metastable C_5A_3 phase. The C_5A_3 phase was also apparent for slag with a CaO/Al_2O_3 ratio of 1.0 and 5 wt pct MgO that were isothermally cooled at 1543 K (1270 °C). Additional phases observed during cooling are considered to be secondary solid phases, which begin to grow when the change in composition of the melt at the solidification front becomes more likely to form these secondary phases. Thermodynamic calculations attempted to determine the phases are precipitated during cooling by using FactSage 6.2 (Thermfact Ltd., Montreal, Canada and GTT Technologies, Aachen, Germany), indicating the C_3MA_2 phase to be the initial primary phase obtained if ternary systems of these compositions are continuously cooled.[16] If the CaO/Al_2O_3 ratio is 1.2, C_3A becomes the dominant phase for both continuous and isothermal cooling conditions. The ternary phase diagram of $CaO\text{-}Al_2O_3\text{-}MgO$ adapted from the literature,[17] given in Figure 11, depicts the phases expected based on the EDS results. This diagram indicates that

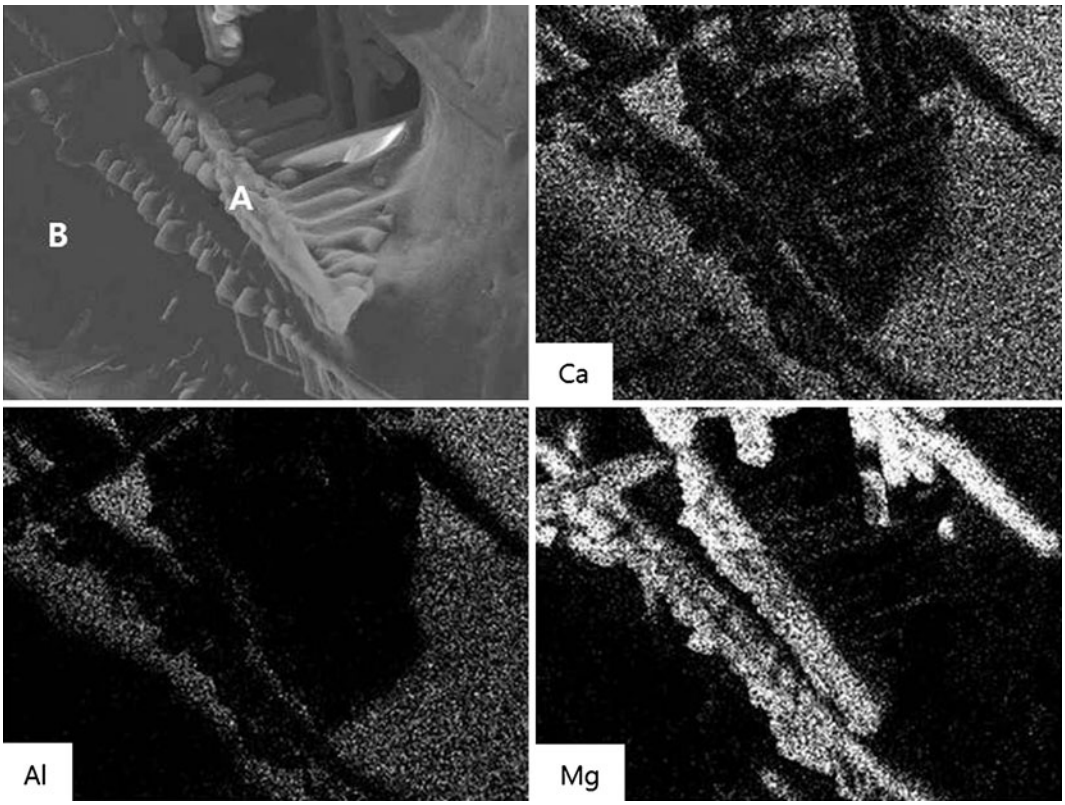

Fig. 15—SEM and EDS mapping images of dendritic MgO phase in the slag at a CaO/Al_2O_3 ratio of 1.0 with 7.5 wt pct MgO cooled at 25 K/min.

Table III. Composition of Primary Crystal Measured by EDS in the Slag of CaO/Al_2O_3 Ratio of 1.0 and 7.5 Weight Percentage MgO Corresponding to Fig. 15

Element	Part A (Wt Pct)	Part B (Wt Pct)
0	50.93	65.24
Mg	44.21	3.29
Al	2.12	19.4
Ca	2.73	12.07

increasing MgO from 5.0 to 7.5 wt pct has negligible effect on the distribution of elements when the cooling rate exceeds 100 K/minutes. According to previously determined values obtained by Rankin and Merwin,[17] slag with MgO approximately above 8 wt pct has MgO as the primary phase when CaO and Al_2O_3 are present in the same amounts. The mapping image of the dendrites in the slag at a CaO/Al_2O_3 ratio of 1.0 with 7.5 wt pct MgO shown in Figure 15 presents evidence of MgO to be the primary phase. The EDS analysis is provided in Table III. Slowly cooled slag is depleted of Mg as the MgO primary phase is precipitated, and C_5A_3 phase becomes the most stable phase instead of C_3MA_2. At higher cooling rates, C_3MA_2 is created as the primary phase.

B. *Crystal Morphology*

Investigation into the shape of the crystal surface was performed *via* the combination of *in situ* observations during crystal growth using confocal microscopy and SEM analysis of as-quenched samples. Slag with a CaO/Al_2O_3 ratio of 1.2 and 5 wt pct MgO, as shown in Figure 16, revealed different nucleation sites and crystal morphologies during isothermal cooling at different temperatures. At 1563 K (1290 °C), as shown in Figure 15(a), a faceted interface grew slowly from the wall of the Pt crucible, and the shape of the crystal remained unaltered for 30 minutes. At 1543 K (1270 °C), as shown in Figure 15(b), a faceted crystal appeared at homogeneous nucleation sites, and dendritic crystals quickly grew on the faceted surfaces as secondary crystals after approximately 20 seconds. At 1543 K (1260 °C), as shown in Figure 15(c), an isotropic dendritic crystal was found in the center of the slag melt, and its shape did not change for 30 minutes. As the experimental temperature decreases, or with higher undercooling, the faceted interfaces become unstable and change into dendritic crystals.[7,18] At an intermediate temperature of 1543 K (1270 °C), the faceted crystal assumed to be C_3A grows and the degree of constitutional supercooling increases with continuous precipitation of C_3A as the liquidus temperature rises, which thus accelerates dendritic growth to increase the surface area for higher heat extraction. Considering the characteristics of the CLSM, a temperature gradient exists between the crucible wall and the melt. This gradient becomes larger at higher temperatures because radiation is focused on the melt surface, and the

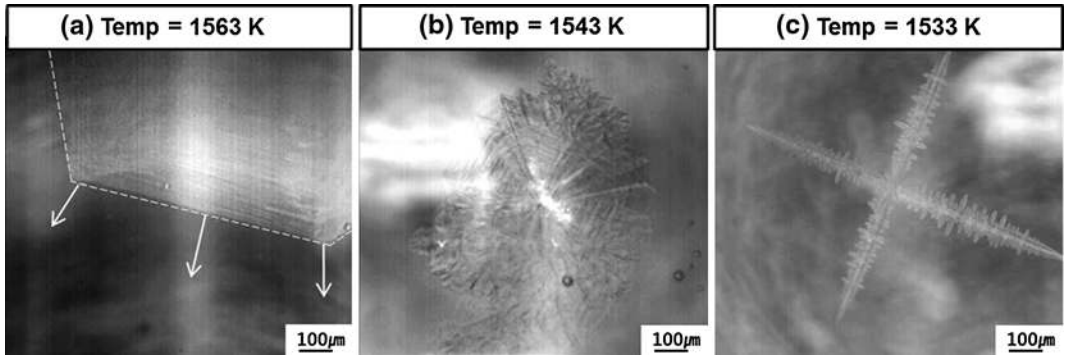

Fig. 16—Confocal images of a slag with $C/A = 1.2$ and 5 wt pct MgO during isothermal cooling at (*a*) 1563 K (1290 °C), (*b*) 1543 K (1270 °C) and (*c*) 1533 K (1260 °C).

driving force for conductive heat transfer through the Pt crucible compared to the melt is greater. Because the liquid melt itself does not have enough supercooling or driving force to give rise to homogeneous nucleation, heterogeneous nucleation can be observed during the experiment. Thus, lower temperatures are required to obtain a degree of supercooling that provides sufficient driving force for nucleation without heterogeneous sites.

V. CONCLUSIONS

TTT/CCT diagrams were obtained, and the identification of the primary crystal phase was accomplished by a combination of CLSM, SEM-EDS and XRD analyses. For slag at a CaO/Al_2O_3 ratio of 1.0 isothermally cooled, 5 wt pct MgO resulted in the shortest incubation time for the crystal formation, and higher crystallization temperatures were observed with the addition of MgO. When slowly cooled, the morphology of the primary crystal in the slag with a CaO/Al_2O_3 ratio of 1.0 and 5 wt pct MgO was an equiaxed faceted crystal, while dendritic primary crystals were observed at all the other MgO contents. Crystals in rapidly cooled specimens are finely dispersed with various shapes, such as spherical nodules, faceted polygonals, needles, and dendrites with higher CaO/Al_2O_3 ratios. During continuous cooling, increased basicity led to a change in the primary phase from C_3MA_2 at a CaO/Al_2O_3 ratio of 0.8 and 1.0 to C_3A at a CaO/Al_2O_3 ratio of 1.2. Increased MgO content from 2.5 to 7.5 wt pct resulted in the alteration of the primary crystal from C_3A to MgO monoxide.

ACKNOWLEDGMENTS

This study was partially supported by the Ministry of Knowledge Economy Project No. 2011-8-1454.

REFERENCES

1. G. Agarwal, K. Hong, M. Fletcher, and R. Speger: *J. Non-Cryst. Solids*, 1991, vol. 130, pp. 187–97.
2. R. Taylor and K.C. Mills: *Ironmaking Steelmaking*, 1988, vol. 15, pp. 187–94.
3. J.W. Cho, T. Emi, H. Shibata, and M. Suzuki: *ISIJ Int.*, 1998, vol. 38, pp. 834–42.
4. J.W. Cho and H. Shibata: *J. Non-Cryst. Solids*, 2001, vol. 282, pp. 110–17.
5. H. Ryu, Z. Zhang, J. Cho, G. Wen, and S. Sridhar: *ISIJ Int.*, 2010, vol. 50, pp. 1142–50.
6. Z. Zhang, G. Wen, and Y. Zhang: *J. Min. Met. Mater.*, 2011, vol. 18, pp. 150–58.
7. J. Huelens, B. Blanpain, and N. Moelans: *J. Eur. Ceram. Soc.*, 2011, vol. 31, pp. 1873–79.
8. F. Engstrom, D. Adolfsson, Q. Yang, C. Samuelsson, and B. Bjorkman: *Steel Res. Int.*, 2010, vol. 81, pp. 362–71.
9. M. Tossavainen, F. Engstrom, Q. Yang, N. Menad, and M. Lidstrom: *Waste Manag. (Oxford)*, 2007, vol. 27, pp. 1335–44.
10. Y. Kashiwaya, C. Cicutti, A. Cramb, and K. Ishii: *ISIJ Int.*, 1998, vol. 38, pp. 348–56.
11. C.T. Mutale, T. Claudon, and A.W. Cramb: *Metall. Mater. Trans. B*, 2005, vol. 36B, pp. 417–18.
12. D.R. Uhlmann and H. Yinnon: *Glasses Science and Technology*, Academic Press, New York, 1983, pp. 1–47.
13. I.H. Jung, S.A. Decterov, and A.D. Pelton: *J. Phase Equilib. Diffus.*, 2004, vol. 25, pp. 329–45.
14. M.G. Vincent and J.W. Jeffery: *Acta Crystallogr. B*, 1978, vol. 34, pp. 1422–28.
15. E. Hagen, Y. Yu, T. Grande, R. Høier, and M.A. Einarsrud: *J. Am. Ceram. Soc.*, 2002, vol. 85, pp. 2971–76.
16. C.W. Bale, A.D. Pelton, and W.T. Thompson, *Factsage*, Ecole Polytechnique, Montreal, 2002, http://www.crct.polymtl.ca.
17. G.A. Rankin and H.E. Merwin: *J. Am. Chem. Soc.*, 1916, vol. 38, pp. 568–88.
18. C. Orrling, S. Sridhar, and A.W. Cramb: *ISIJ Int.*, 2000, vol. 40, pp. 877–85.